



# Tropospheric NO<sub>2</sub> concentrations over West Africa are influenced by climate zone and soil moisture variability

Ajoke R. Onojeghwo<sup>1\*</sup>, Heiko Balzter<sup>1, 2</sup>, Paul S. Monks<sup>3</sup>

<sup>1</sup>University of Leicester, Centre for Climate Research, University Road, Leicester, LE1 7RH

5 <sup>2</sup>National Centre for Earth Observation, University of Leicester, University Road, Leicester, LE1 7RH

<sup>3</sup>University of Leicester, Department of Chemistry, University Road, Leicester, LE1 7RH

Correspondence to: Ajoke R. Onojeghwo ([arool@le.ac.uk](mailto:arool@le.ac.uk), [a.onojeghwo@gmail.com](mailto:a.onojeghwo@gmail.com))

10

## Abstract.

The annual cycles of soil moisture and NO<sub>2</sub> have been analysed across the climate zones of West Africa using two satellite data sets (OMI on AURA and ASCAT on MetOp-A). Exploring the sources and sinks for NO<sub>2</sub> it is clear that the densely populated urban cities including Lagos and Abuja had the highest mean NO<sub>2</sub> concentrations ( $>1.8 \times 10^{15}$  molecules cm<sup>-2</sup>) indicative of the anthropogenic urban emissions. The data analysis shows that rising soil moisture levels may influence the sink of NO<sub>2</sub> concentrations after the biomass burning. The results also show significant soil moisture changes in areas of high humidity especially in the east equatorial monsoon climate zone where most of the Niger delta is located (4 %/yr.). A decline in NO<sub>2</sub> (0.9 %/yr.) was also observed in this climate zone. Beyond seasonal linear regression models, climate based Granger's causality tests show that tropospheric NO<sub>2</sub> concentrations from soil emissions in the arid steppe (Sahel) and arid desert climate zones of West Africa are significantly affected by soil moisture variability ( $F > 10$ ,  $p < 0.01$ ). The arid steppe and arid deserts regions showed no significant changes in soil moisture levels but significant increase in tropospheric NO<sub>2</sub> concentrations ( $> 0.8$  %/yr.). The results demonstrate the critical sensitivity of the West African emissions of NO<sub>2</sub> on soil moisture and climate zone.

15

20

## 25 1 Introduction

Nitrogen oxides (NO<sub>x</sub>) play critical roles in many atmospheric processes including the catalytic production of tropospheric ozone and the formation of nitric acid being key elements of local air quality with effects felt across global tropospheric chemistry (Richter et al., 2005). Atmospheric pollution affects human and ecosystem health as well as being intrinsically linked to climate in the present and coming decades (von Schneidemesser et al., 2015). NO<sub>2</sub> is a pollutant and key precursor for tropospheric Ozone (O<sub>3</sub>) formation (Monks et al., 2015) and has both anthropogenic (fossil fuel / bio-fuel burning and incomplete combustion) and natural sources (soil emissions). West Africa is known to generate large amounts of pollutants from both its megalopolis concentrated around the Gulf of Guinea (Hopkins et al., 2009) and from biomass burning episodes during the Northern hemisphere dry season (Pradier et al., 2006) which occurs before the planting/rainfall season (Ker,

30



1995). Urban vehicular pollution is also rather high in urban West Africa owing to the high usage of often poorly maintained second hand cars and low quality fuel (Schwela, 2009). It has been estimated that in addition to seasonal biomass burning which releases  $\text{NO}_2$  and pyrogenic carbon into the atmosphere (Lehsten et al., 2009) directly, soil emissions of  $\text{NO}_x$  represent 15% of global N emissions (Hudman et al., 2012).

5

Soil moisture conditions are an aggregated expression of the hydrological regime in the area which encompasses rainfall, evapotranspiration, surface runoff and groundwater supply (Ibrahim et al., 2015). Soil moisture trends affect the nitrogen (Keller and Reiners, 1994) energy, water and carbon exchange processes between the land surface and atmosphere (Basara and Crawford, 2002). It is also a determinant of the type and condition of vegetation in addition to overall ecosystem health in a region (GCOS, 2015). Over parts of West Africa, decadal-scale trends in rainfall have been analysed and showed flooding in the western Sahel between 2008 and 2010 (Hoscilo et al., 2015). Information on the temporal dynamics of soil moisture is important to identify the start of the wet season and drought events, especially in semi-arid/Sahel regions, where vegetation growth is driven by soil moisture variations (Ibrahim et al., 2015). IPCC (2007) projected that the effect of climate change on soil moisture will vary with soil characteristics, such that soils with lower moisture retention capacity (as found in regions of aridity) will have greater sensitivity and vulnerability to climate change. The Global Climate Observing System (GCOS) has defined soil moisture as an essential climate variable (ECV) which can be monitored at a regional and global scale from satellites measurements validated from a network of in-situ measurements (GCOS, 2015).

Some researchers have found large emissions of rain-induced  $\text{NO}_x$  ( $\text{NO} + \text{NO}_2$ ) from the soil following long periods of drought in savannahs and seasonally dry forests (Jaegle et al., 2005; Feig et al., 2008; Hudman et al., 2010; Kim et al., 2012) and a strong link between this soil-released  $\text{NO}_x$  and atmospheric  $\text{NO}_2$  (Jaegle et al., 2005; Delon et al., 2015). Microbial activities lead to denitrification and nitrification in the soil, resulting in the formation of soil gases such as  $\text{NO}$  (Delon et al., 2015). Kim et al. (2012) explained that root secretions from reviving plants following rewetting could significantly affect the soil surface flux of soil gases like  $\text{NO}$ . Water-stressed bacteria become active as soon as water drops on the dry soil (Hudman et al., 2012) and feed on nutrients which have accumulated in dry season or longer periods between irregular/sporadic rainfalls (Meixner and Yang, 2006).  $\text{NO}$  is also produced rapidly after N (Nitrogen) fertilizers (both livestock manure and synthetic fertilizer) are applied to the soil to improve agricultural outputs (Pilegaard, 2013). The  $\text{NO}$  emissions from these microbial/bacterial activities and nitrification of the soil through fertilizers are released to the atmosphere through pulsing and oxidised in a reaction with  $\text{O}_3$  in the atmosphere to form  $\text{NO}_2$  (Pilegaard, 2013) especially in strongly sunlit areas of semi-aridity (Delon et al., 2008). It has been predicted that by the 2050s, soil emissions of  $\text{NO}_x$  are likely to decline by 9% in Northern (West and North) Africa while biomass burning emissions will be 12% more (Wai et al., 2014).



The West African region is situated between 4° N and 28° N latitude and 16° W and 15° E longitude, covering a total area of 6 million km<sup>2</sup> (one fifth of Africa) with the Gulf of Guinea as its southern boundary. The seasonal oscillation of the ITCZ (inter-tropical convergence zone) in the north-south direction over West Africa defines the climate zones (Conway, 2009) as it determines how much rainfall each climate zone gets annually. The Köppen-Geiger climate zones of West Africa (Kottke et al., 2006), which occur in latitudinal strata as shown in Figure 1 are:- the equatorial monsoon zone, equatorial winter zone, arid steppe zone and arid desert zone.

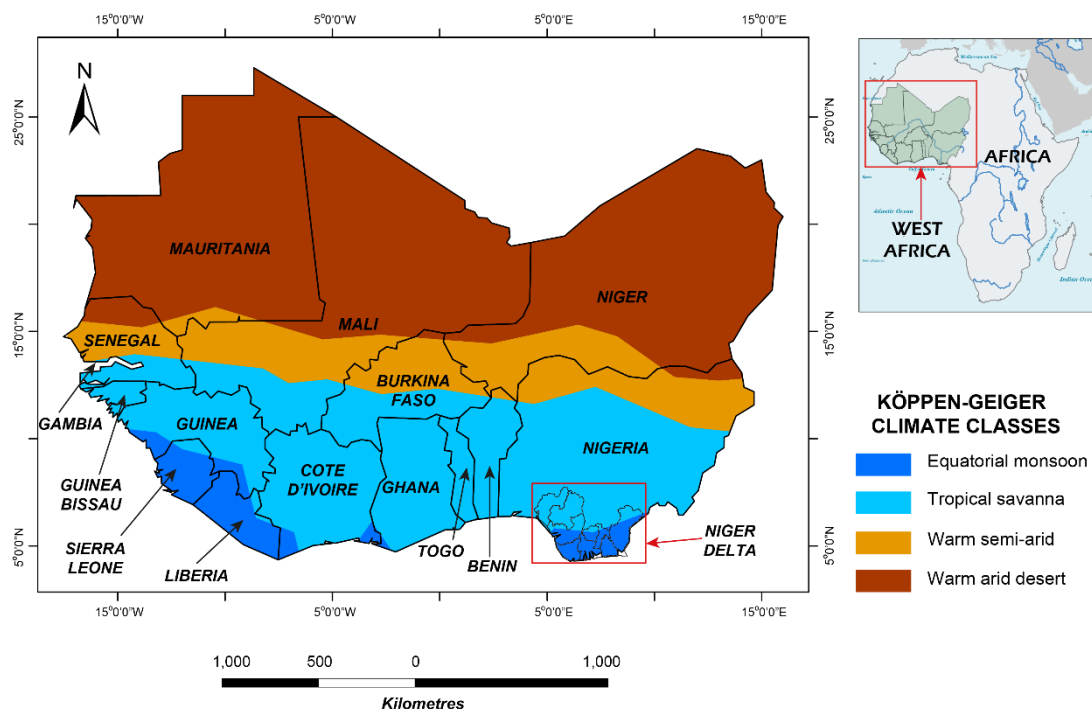


**Figure 1: A map of West Africa showing the climate zones. The equatorial monsoon region is found along the West African boundary with the Gulf of Guinea. The arid steppe zone is often referred to as the Sahel.**

10 The annual rainfall over different zones is relatively constant but decreases from south to north away from the equator (Eltahir and Gong, 1996). However, drought and subsequent floods have been experienced in West Africa over the last few decades especially since 2002 (Tschakert et al., 2010), altering the annual rainfall cycles. Based on temperature and rainfall, there are two main seasons (dry and wet) in the humid areas of West Africa. These patterns vary for the semi-arid (arid steppe) / arid (arid desert) regions which have three main seasons:- a cool dry season between October and February, a warm dry season between March and June, and a warm wet season between July and September (Batello et al., 2004). In the other climate zones, there is one main dry season from November to February (the fire season is usually at its peak from December to February) and one main wet season: from June to August, with intermittent rainfall before and after the main wet season.

15 FAO (1983) identifies two air masses which control rainfall and atmospheric transport around West Africa: the tropical



maritime (characterized by south-westerly winds coming to land off the Gulf of Guinea and bearing moisture) in the wet season and the tropical continental (originating from the Sahara desert bearing dryness) in the dry season.

In addition to climate variability, land/vegetation cover types may affect the soil-atmosphere exchange rates of soil NO<sub>x</sub> (Feig et al., 2008). Figure 2 shows the percentage land cover of the West African climate zones aggregated from the ESA GLOBCOVER 2009 (Bontemps et al., 2010) land cover map. The equatorial climate zone was split into three subsets based on the location within West Africa (west, central and east equatorial monsoon). The equatorial winter region has the highest urban land cover spread across the zone and the West African coast including Abuja, Lagos, Accra and Dakar megacities. In addition to vast bare areas and sparse vegetation like in the arid desert zone (> 25 %), the arid steppe zone has the largest percentage of regularly flooded vegetation (~ 4%) and rain-fed croplands (10 %) which are strongly affected by rainfall/soil moisture seasonality. The equatorial monsoon zones are covered by 25 – 30% broadleaved deciduous forests. The east equatorial monsoon with consists of the biodiverse wetlands of the Niger Delta has the highest percentage of wetlands (broadleaved flooded forest).

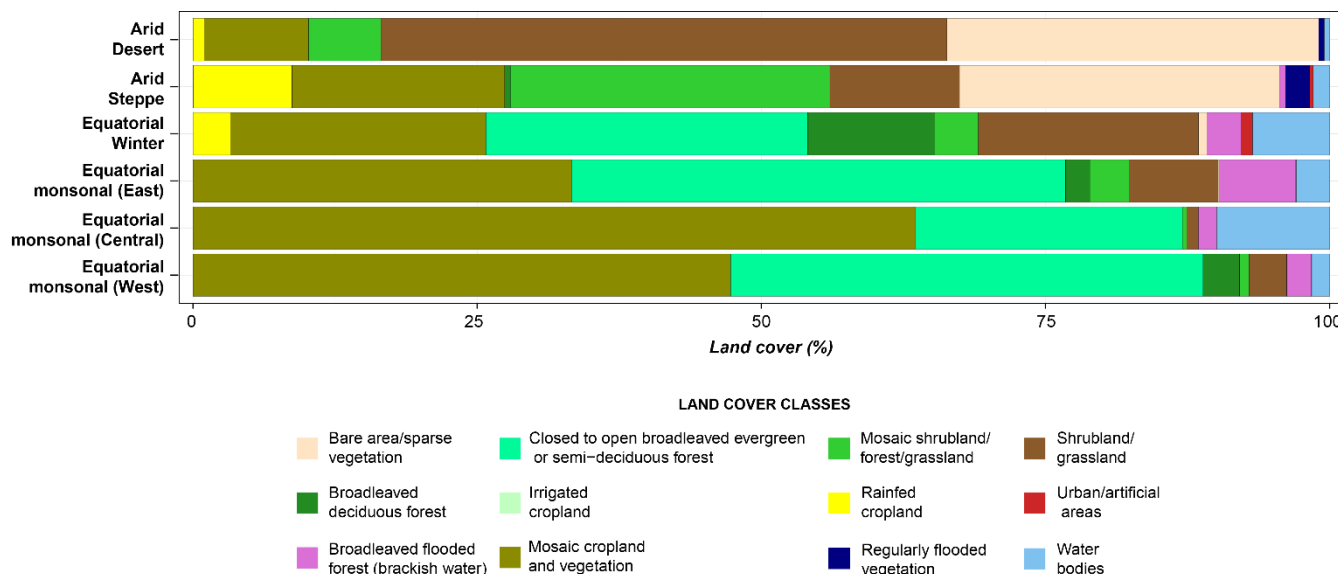


**Figure 2. Percentage land cover over the West African climate zones. The equatorial monsoon region includes the highest urban/artificial areas. The East equatorial monsoon zone has most of the broadleaved flooded forest.**

Several factors affect the atmospheric concentrations of NO<sub>2</sub> over West Africa. The aim of this study was to investigate the seasonality and co-variation of NO<sub>2</sub> and soil moisture using satellite data and to assess the influence of climatology and soil moisture seasonality on the seasonal dynamics of NO<sub>2</sub> over West Africa. It uses remotely sensed soil moisture and NO<sub>2</sub> data



from OMI on-board AURA and ASCAT on-board MetOp-A respectively to model the seasonal effects of soil moisture content on tropospheric abundance of NO<sub>2</sub> during a 7-year period (December 2007- November 2014).

## 2 Experimental

### 5 2.1 Data

#### 2.1.1 OMI NO<sub>2</sub> tropospheric vertical columns

Satellite measurements of the troposphere make it possible to retrieve local, regional and global data beyond previously available ground-based measurements (Monks and Beirle, 2011). The OMI spectrometer is a Dutch instrument with a spatial resolution of approximately 13 × 24 km at nadir in normal operational mode. A major advantage of OMI over similar instruments retrieving pollutant concentrations is the capacity to measure important trace gases with a small footprint and daily global coverage (Levelt et al., 2006) thus aiding the identification of local emission sources of such gases. MAX-DOAS in-situ observations from ground stations have been used to validate OMI NO<sub>2</sub> retrievals for example, in southern France, China and Asia (Schneider, 2015) and showed good agreement with in situ observations over rural areas where soil moisture plays a vital role in atmospheric abundance of NO<sub>2</sub>. Lamsal et al. (2014) evaluated OMI retrievals using in-situ near surface observations and MAX DOAS in Japan using one remote and another urban site. The authors found OMI and MAX DOAS NO<sub>2</sub> retrievals to be consistent ( $r = 0.86$ ) with a larger negative bias in the urban site. NO<sub>2</sub> column concentrations are retrieved from OMI using the differential optical absorption spectroscopy (DOAS) and its modifications (Oetjen et al., 2013). Hudman et al. (2010) analysed the variability of soil nitric oxide around a non-irrigated agricultural land using OMI and GEOS-Chem measurements. They found that OMI NO<sub>2</sub> products captured peak pulsing episodes over agricultural lands better than the model which showed pulsing events occurred longer than they actually did.

Daily gridded data from the version 2.1 of the level 3 OMI tropospheric NO<sub>2</sub> product (OMNO2d), at a resolution of 0.25° x 0.25° (available at <http://mirador.gsfc.nasa.gov/>) was used for monthly NO<sub>2</sub> pollution levels. The cloud-screened tropospheric OMNO2d dataset was used as most pixels used in the retrieval process have cloud fraction < 30 % (OMI-NO2-Algorithm-Team, 2013) and data bias is minimal (Grajales and Baquero-Bernal, 2014).

#### 2.1.2 ASCAT Soil Water Index

The Copernicus Soil Water Index (SWI) product from ASCAT(Advanced SCATterometer) instrument on MetOp-A and MetOp-B was developed for applications within the framework of the GMES project GEOLAND2 to provide a modelled profile estimate of soil moisture conditions at different depths using satellite data as input (Kidd et al., 2014). The soil water index product is generated by using repeat cycles of surface soil moisture conditions retrieved by ASCAT (a C-band real-aperture radar sensor) to estimate the profile soil moisture content (Wagner et al., 2013). SWI is retrieved with a daily time



step for mid-latitude regions such as parts of Europe and West Africa and is suitable for soil moisture estimation in these areas (Brocca et al., 2010). SWI showed good agreement with most global in-situ soil moisture observations stations but deteriorates with influences of topography, water fraction, noise and also in situ observation depth (Paulik et al., 2014).

- 5 The 10-day ASCAT (MetOp-A) SWI data Version 3 was downloaded from the Copernicus global land service (<http://land.copernicus.vgt.vito.be>) for all available depths. The SWI data near the surface up to a depth of 5cm is approved by the GCOS as an indication of surface soil moisture. The SWI data at a depth of 5cm (T005) was chosen for analysis as it showed better data retrieval quality (> 75 %) over West Africa relative to the data quality for 1cm was < 50 %. The SWI data set (originally gridded at 0.1° x 0.1°) was aggregated to 0.25° x 0.25° to ensure uniformity with the OMNO2d data set.

## 10 2.2. Methods

All data sets were analysed using the freely available statistical programming language R (The R Core Team, 2014). R packages used in data manipulation were “rhd5” (Fischer and Pau, 2015), “ncdf4” (Pierce, 2015) “lattice” (Sarkar, 2015), “zoo” (Zeileis and Grothendieck, 2005), “raster” (Hijmans, 2015), “visreg” (Breheny and Burchett, 2013) and “lmtest” (Hothorn et al., 2014). The S-G (Savitzky-Golay) algorithm was used to eliminate false peaks from the gridded SWI and  
 15 NO<sub>2</sub> time series. This is a simplified least-squares-fit convolution for smoothing and computing derivatives of a set of consecutive values (Savitzky and Golay, 1964; Chen et al., 2004). It improves the results of time series analysis by following trends at scales dictated by the interplay between the defined order of the polynomial and the size of the filter’s footprint in the data (Thornley, 2007). Stevens and Ramirez-Lopez (2014) define the S-G fit as a local polynomial regression on a signal which requires equidistant bandwidth and they express in Eq. (1) mathematically as:

$$20 \quad X_{j^*} = \frac{1}{N} \sum_{h=-k}^k C_h X_{j+h}, \quad (1)$$

where  $X_{j^*}$  is the new value,  $N$  is a normalizing coefficient,  $k$  is the number of neighbour values at each side of  $j$  and  $C_h$  are pre-computed coefficients that depend on the chosen polynomial order and degree (smoothing, first and second derivative). The S-G algorithm has been used to filter time series such as vegetation index data (Erasmí et al., 2006) with results  
 25 indicating the high potential of S-G filtering to minimize noise while conserving original properties of time-series. A pixel-wise S-G filter was used to smooth out unnecessary noise in the NO<sub>2</sub> and SWI time series to enable identification of both primary and secondary peaks annually. A third-order polynomial using 5 neighbourhood values was used in the filtering process to preserve seasonality. The NO<sub>2</sub> and SWI data sets were then subset based on vector data of the Köppen Geiger climate zones of West Africa. The equatorial monsoon climate zone was split in 2 regions based on location relative to the  
 30 equatorial winter region (West and East equatorial monsoon regions) The central parts of the equatorial monsoon zone wasn’t considered as this is a relatively small area (< 30,000 km<sup>2</sup>).



Monthly mean aggregates were created for time series analysis. Bean plots were then used to visualize the inter-regional climate-based statistical differences in NO<sub>2</sub> and SWI distributions. Annual means were aggregated from monthly climate zone based means and then normalised to the 2007/08 annual mean to analyse percentage changed between 2007 and 2014. A cumulative percentage change was also determined for each climate zone. The monthly time series were grouped for

5 annual quarters based on months for seasonal regression analysis into DJF (December, January and February), MAM (March, April and May), JJA (June, July and August) and SON (September, October and November). The climate zone-based seasonal relationships between soil moisture and NO<sub>2</sub> were then analysed using linear regression models to test if soil moisture variations affect NO<sub>2</sub> concentrations in anyway. For each season, all monthly data were used directly without a seasonal aggregate.

10 While linear regression models explain the relationships between entities either at a point in time or within a time lag, they do not in themselves allow inference of the cause-effect relationships between entities. Knowledge of these causal relationships gives a measure of understanding and a sense of potential ability to predict the consequences of actions that have not yet been performed (Pearl, 2000). The Granger causality (GC) was developed to improve the identification of the direction of causality between two related variables while checking for occurring feedback (Granger, 1969). It uses

15 predictability as opposed to regression to identify causation between time-series variables (Sugihira et al., 2012). GC tests whether any past values of an explanatory variable in a time series of two variables can add to the explanatory autoregressive model. Granger-causality must not be confused with causality in the sense of a cause-effect relationship. The Granger-causality of soil moisture on NO<sub>2</sub> concentrations was tested for each climate zone using monthly mean at a one-month lag.

20 The moving averages for time series was computed for a period of twelve months for each time stamp in the time series. This was computed with the formula in Eq. (2) below:

$$MA_{tn} = \frac{1}{n} * \sum_{i=0}^{n-1} C_{t-i}, \quad (2)$$

where  $MA_{tn}$  is the moving average for a time  $t$  in the series,  $C_t$  is the value for time  $t$  and  $n$  is the number of months considered in the moving average;  $n$  was taken to be 12 (6 before and 6 after) for all months in the year. Anomalies in the

25 time series of NO<sub>2</sub> and soil moisture were then analysed from the moving average time series using the formula in Eq. (3) below:-

$$A_i = \left( \frac{1}{n} * \sum_{t=1}^n MA_t \right) - MA_t, \quad (3)$$

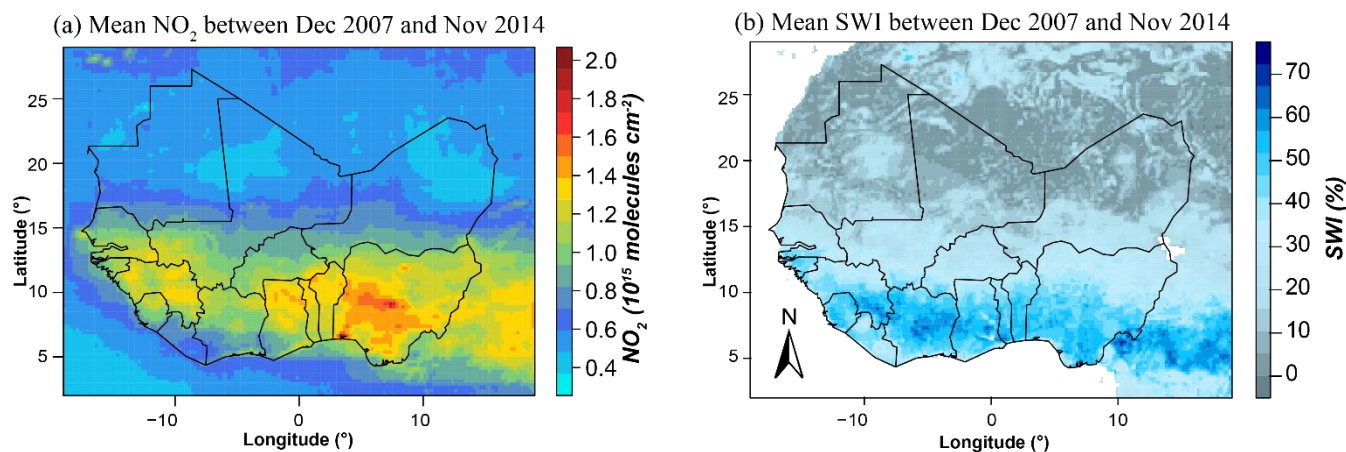
Where  $A_i$  is the anomaly at time  $t$ ,  $n$  is the length of the time series and  $MA_t$  is the moving average at time  $t$ . This was to see how soil moisture and NO<sub>2</sub> variability occurred within the 7-year period. To remove autocorrelation in the time series,

30 climate based annual means of NO<sub>2</sub> and SWI were used for normalised trend and percentage change analysis.



### 3 Results and discussions

A pixel-wise 7-year mean of tropospheric NO<sub>2</sub> concentrations (Figure 3a) showed highest concentrations in the densely populated Nigerian cities, Abuja and Lagos ( $>1.8 \times 10^{15}$  molecules cm<sup>-2</sup>) where urban vehicular emissions affect tropospheric NO<sub>2</sub> strongly. Mean concentrations over large areas where biomass burning is the main source of anthropogenic NO<sub>2</sub> were between 1.2 and  $1.5 \times 10^{15}$  molecules cm<sup>-2</sup>. Areas where soil moisture emissions were a major factor affecting atmospheric concentrations of NO<sub>2</sub> had slightly lower concentrations ( $< 1.2 \times 10^{15}$  molecules cm<sup>-2</sup>). With soil moisture (Figure 3b), SWI levels followed a South to North gradient with similar levels along the East-West latitudinal boundaries across West Africa except in the arid desert climate zone. The arid desert zone had low mean SWI levels  $< 10\%$  over most areas while central Cote d'Ivoire had the highest mean soil moisture levels (SWI  $> 60\%$ ). Most areas with soil moisture  $\geq 55\%$  had a mixture of broadleaf deciduous forest, shrublands and grasslands. Most areas in the equatorial winter and equatorial monsoon zones had soil moisture levels  $> 40\%$ . In the arid steppe climate zone, mean soil moisture was about 30%.

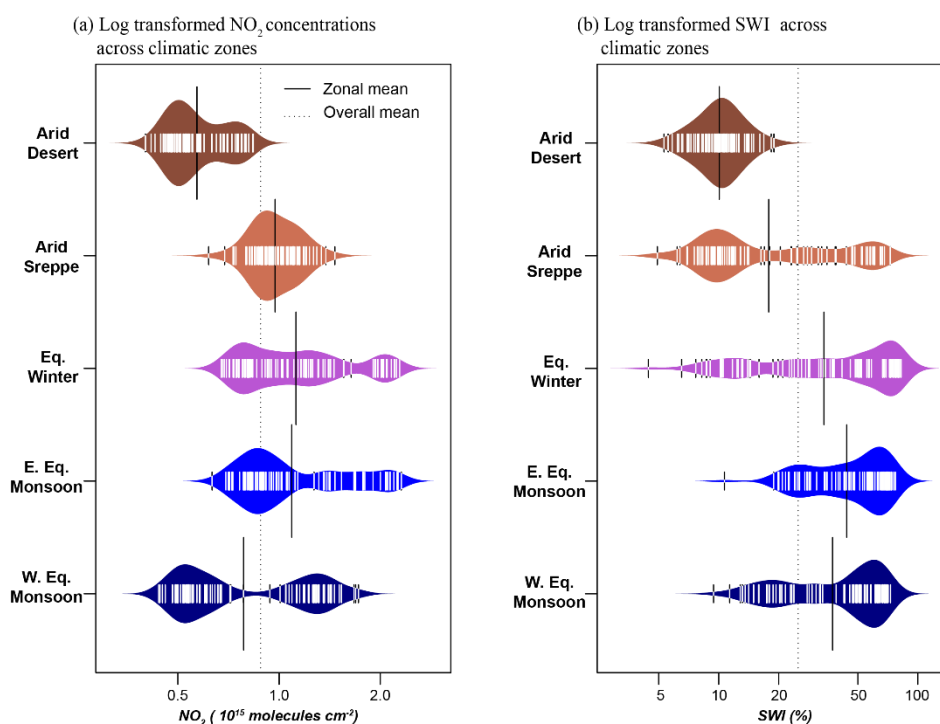


3. Overall mean values of (a) cloud corrected tropospheric NO<sub>2</sub> and (b) soil moisture levels between December 2007 and November 2014. Abuja and Lagos (Urban areas) had the highest NO<sub>2</sub> concentrations. Central Cote d'Ivoire had the highest mean soil moisture levels during the period considered.

Figure 4a shows the statistical distribution of NO<sub>2</sub> concentrations across the West African climate zones. The mean monthly NO<sub>2</sub> concentrations in the east equatorial monsoon and equatorial zones were similar (between  $0.7$  and  $2.3 \times 10^{15}$  molecules cm<sup>-2</sup>) and had a mean of  $1.0 \times 10^{15}$  molecules cm<sup>-2</sup>. Both climate zones are greatly affected by anthropogenic emissions (air pollution in the equatorial winter zone is greatly affected by urban emissions and by oil exploration/gas flaring in the east equatorial zone). In the West equatorial zone where biomass burning is the main driver of NO<sub>2</sub> pollution, a clearly bi-modal distribution in NO<sub>2</sub> concentrations was observed. NO<sub>2</sub> was mostly below the West African mean ( $0.9 \times 10^{15}$  molecules cm<sup>-2</sup>) in the arid desert climate zone. With the arid climate zone, the overall mean NO<sub>2</sub> concentrations ( $1.1 \times 10^{15}$  molecules cm<sup>-2</sup>) was higher than in the west equatorial climate zone but slightly lower than it was in the equatorial winter and east equatorial



monsoon climate zones. With soil moisture (Figure 4b), the highest variability from the zonal mean was observed in the arid steppe climate zone. The arid steppe zone showed bi-modality in soil moisture distribution. Most of the monthly levels in this climate zone were below the zonal mean but the highest observed monthly soil moisture mean (65 %) compared to levels in the equatorial winter and monsoon zones. The arid desert zone showed a normal distribution of soil moisture with all monthly means lower (< 20 %) than the overall West African mean. The equatorial monsoon and winter climate zones showed bi-modal distributions in soil moisture levels and overall means > 40%.



10 **Figure 4. Bean plots showing the statistical distributions of monthly tropospheric NO<sub>2</sub> and soil moisture in the major climate zones of West Africa between December 2007 and November 2014. A clearly bi-modal distribution in NO<sub>2</sub> concentrations and soil moisture levels was observed in the West equatorial monsoon region.**

### 3.1 Annual cycles of tropospheric NO<sub>2</sub> and soil moisture

Figure 5 shows the climate zone based general annual cycles of monthly means and ranges of NO<sub>2</sub> and soil moisture over West Africa. Most climate zones showed one peak in NO<sub>2</sub> concentrations annually which was in December in the equatorial winter (> 2.2 × 10<sup>15</sup> molecules cm<sup>-2</sup>) and equatorial monsoon zones (~ 1.5 – 2.1 × 10<sup>15</sup> molecules cm<sup>-2</sup>). The arid steppe zone showed a primary NO<sub>2</sub> peak in May (~ 1.3 × 10<sup>15</sup> molecules cm<sup>-2</sup>) when atmospheric NO<sub>2</sub> concentrations are driven by soil NO emissions and a secondary peak in October (1.1 × 10<sup>15</sup> molecules cm<sup>-2</sup>) when biomass burning is prevalent. The arid desert zone showed similarity to the trends observed in the arid steppe climate zone but with a lag of one month such that NO<sub>2</sub> was at its peak concentration in June (0.75 × 10<sup>15</sup> molecules cm<sup>-2</sup>), one month after soil moisture began to increase in



the arid steppe zone and a secondary peak in November. The starting months for increase in soil moisture levels varied such that zones closer to the Gulf of Guinea (equatorial winter and east equatorial monsoon) started increasing in February with levels > 20% in the east equatorial winter zone, the West equatorial monsoon in March (> 17%), the arid steppe in May (> 10%) and the arid desert which is furthest in June annually (> 8%). Soil moisture in the West equatorial zone started to increase in March annually (> 15%) at a time when annual biomass burning is still on-going (N'Datchoh et al., 2015). However, despite this biomass burning, the results in Figure 5 show that when soil moisture levels started increasing in March in the west equatorial monsoon zone, tropospheric NO<sub>2</sub> concentrations began to decline ( $< 1.3 \times 10^{15}$  molecules cm<sup>-2</sup>). Soil moisture levels were at zonal peaks in August annually in all climate zones with the Equatorial winter zone having highest soil moisture levels (about 80%). The east equatorial zone, where the highest percentage of broadleaved flooded forest (wetlands) exist, had the highest soil moisture levels between December and May annually (> 20%).

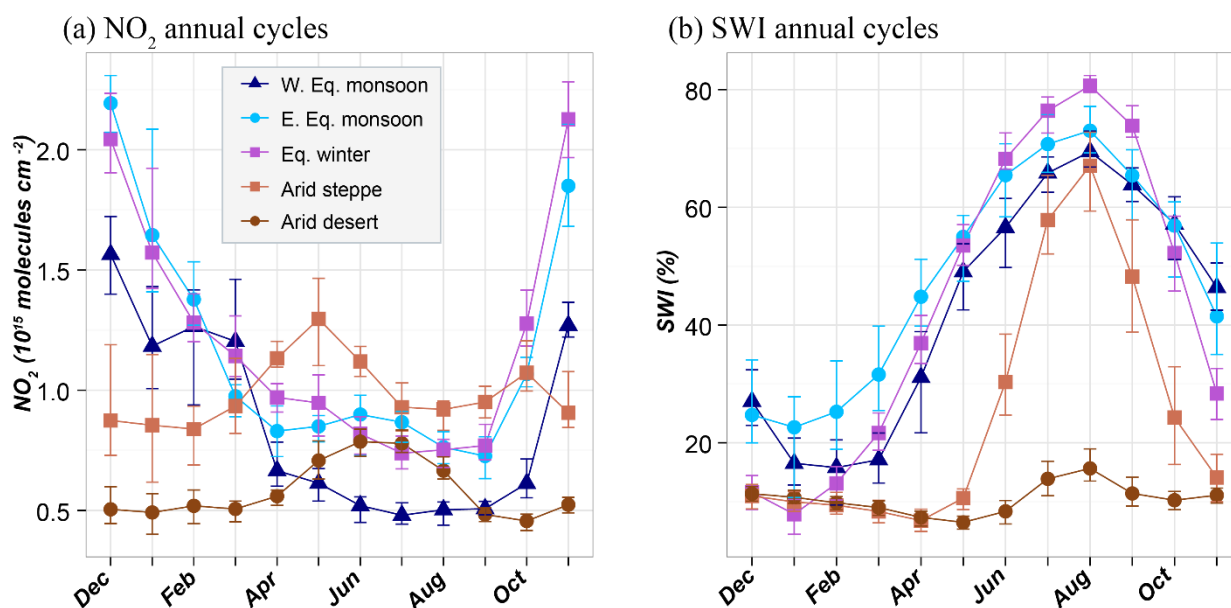


Figure 5. Climate-based monthly means of NO<sub>2</sub> concentrations from OMI and soil water index from ASCAT between December 2007 and November 2014. The peak in NO<sub>2</sub> observed in May occurred when soil moisture began to rise after long periods of dryness. A similar peak in NO<sub>2</sub> (a) was observed in the arid desert climate zone in June when soil moisture began to increase (b).

In the arid steppe zone, the main NO<sub>2</sub> peak was observed in May with the first increase in soil moisture after long periods of dryness. The soil moisture levels showed a gradient of reducing soil moisture levels from South (the equatorial zones) to North (the arid zones) such that highest soil moisture levels were in the equatorial zones (13 – 85%) and lowest in the arid desert zone (5 – 70%). The arid steppe zone had similar soil moisture variability to the arid steppe zone between December and April (5 – 10%) and showed similarity to levels in the equatorial zones (> 30%) between June and November annually



( $0.5 \times 10^{15}$  molecules  $\text{cm}^{-2}$ ). The highest deviation ( $\sim 20\%$ ) from the climate zone mean soil moisture was observed in the east equatorial monsoon zone between February and April.

### 3.2 Seasonal and general effects of soil moisture on $\text{NO}_2$

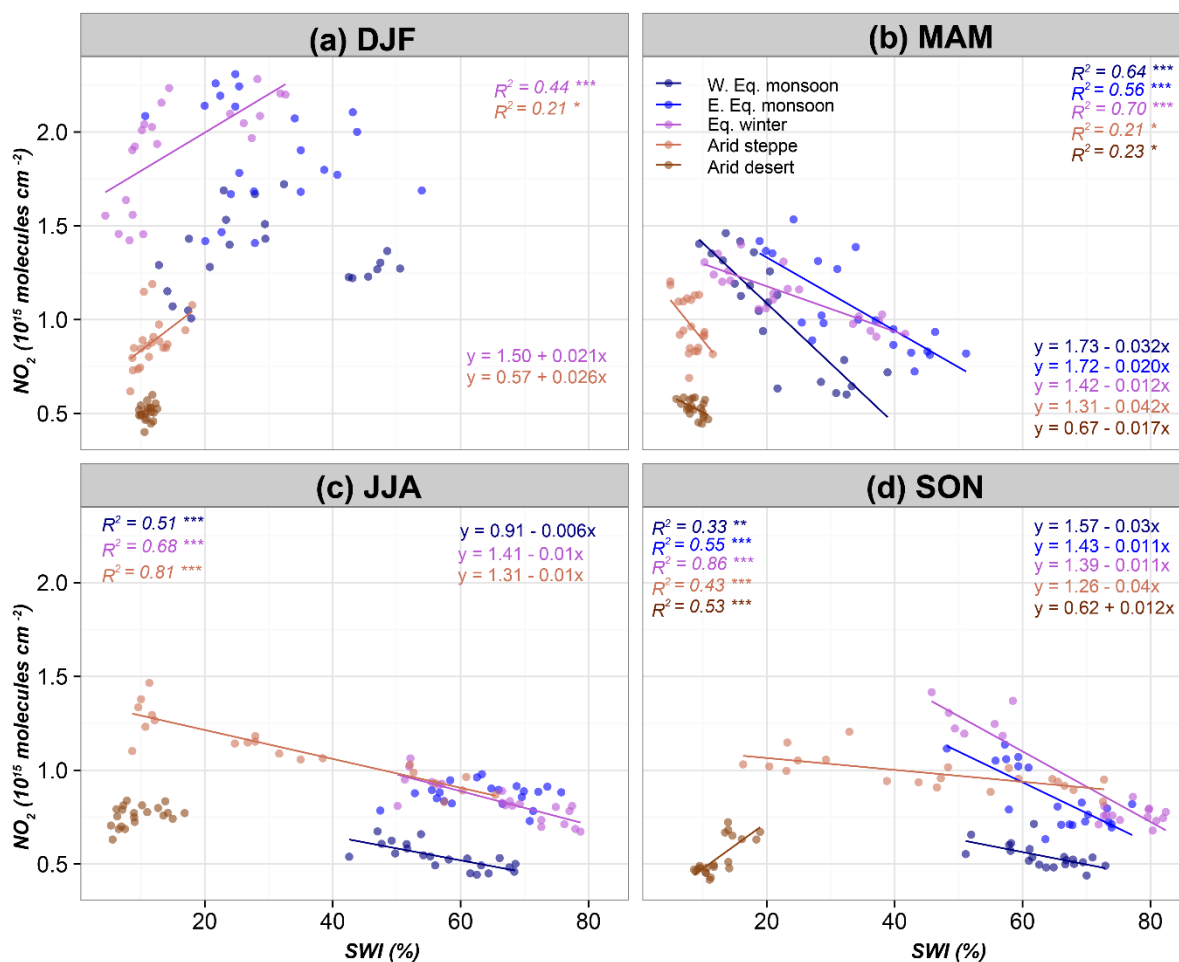
Figure 6 shows the quarterly/seasonal relationships between soil moisture and tropospheric  $\text{NO}_2$ . Each point in the scatterplot corresponds to a month of the year in the particular quarter rather than a seasonal mean. In the DJF season when soil moisture was mainly  $\leq 50\%$ , in most climate zones, variations in soil moisture had no significant relationship with  $\text{NO}_2$  concentrations ( $R^2 < 0.2$ ) except in the equatorial winter zone ( $R^2 = 0.44$ ,  $p < 0.001$ ) and in the arid steppe climate zone ( $R^2 = 0.44$ ,  $p < 0.001$ ). The increase of  $\text{NO}_2$  concentrations with increasing soil moisture contents observed in the DJF season in the equatorial winter zone may be attributed to fuel moisture content during biomass burning episodes rather than soil emissions. The equatorial winter This zone experiences most of the large area biomass burning in West Africa (N'Datchoh et al., 2015) especially around croplands/grasslands. Chen et al. (2010) analysed the effect of moisture on carbon and nitrogen emissions from biomass burning and found that when fuel moisture was high, the combustion efficiency of fires were lower, pre-flame smouldering periods were longer and the flaming phase became shorter. They also believe these processes facilitate the release of  $\text{NO}_x$  into the atmosphere from wet litter composite and certain leaf types. The formation of  $\text{NO}_2$  from  $\text{NO}_x$  released from burning wet litter composite may be responsible for the observed increase in  $\text{NO}_2$  with higher soil moisture levels observed in the equatorial winter zone in the dry season (Figure 6a).

While all equatorial zones had lower  $\text{NO}_2$  concentrations in the MAM season ( $\leq 1.4 \times 10^{15}$  molecules  $\text{cm}^{-2}$ ) than was observed in the DJF season, the arid steppe zone showed no difference in tropospheric  $\text{NO}_2$  concentrations as soil moisture became  $< 10\%$ . Between March and May (MAM), as soil moisture increased, tropospheric  $\text{NO}_2$  declined in most climate zones except in the arid desert where soil moisture remained low until June (Figure 6b). In all climate zones, there were significant effects of soil moisture on declining  $\text{NO}_2$  ( $p < 0.05$ ) except in the arid desert zone. As soil moisture increases, humidity, vegetation greenness and health improves especially in the equatorial monsoon and winter zones where the land cover consists of  $\geq 25\%$  of the broadleaved evergreen/ deciduous forest and  $> 30\%$  mosaic cropland and vegetation classes. The increasing soil moisture can cause an increase in the abundance of the OH radical a key loss process for  $\text{NO}_2$  (see Monks (2005)).

Figure 6c shows the regression between soil moisture and  $\text{NO}_2$  between June and August (JJA). In the JJA season when soil moisture was at its peak in all climate zones, soil moisture levels had no significant effect on  $\text{NO}_2$  concentrations in the east equatorial and arid climate zones.  $\text{NO}_2$  concentrations were highest in the arid steppe zone relative to other climate zones  $\text{NO}_2 (\geq 1.0 \times 10^{15}$  molecules  $\text{cm}^{-2})$  when soil moisture was  $\leq 10\%$ . When soil moisture levels became  $\geq 20\%$  in the arid steppe climate zone, a clearly negative regression ( $R^2 > 0.81$ ,  $p < 0.001$ ) with  $\text{NO}_2$  was observed with concentrations declining as moisture levels increased. The high  $\text{NO}_2$  concentrations when soil moisture is  $< 10\%$  is attributed to the oxidation of soil released NO as dry soils especially in the West African Sahel are rewetted after long periods of dryness (Pilegaard, 2013; Delon et al., 2015). Hudman et al. (2012) notes that in many models, the period of soil  $\text{NO}_x$  pulsing is



misrepresented as being longer than detected from OMI NO<sub>2</sub> products. All climate zones except the arid desert zone showed a decline in NO<sub>2</sub> with increasing soil moisture in the JJA season as NO<sub>2</sub> concentrations continued to rise soil moisture ≤ 20 % in the JJA season.



5

**Figure 6: Linear models showing seasonal relationships between soil moisture and NO<sub>2</sub> from (a) December to February (b) March to May (c) June to August and (d) September to November with stated adjusted R<sup>2</sup> values. Only significant regression lines are shown. Tropospheric NO<sub>2</sub> declined significantly when soil moisture was > 20% between March and August.**

10

The negative relationship between soil moisture and NO<sub>2</sub> ( $p < 0.001$ ) continued in all climate zones in the SON season except in the arid desert zone (Figure 6d). The soil moisture/NO<sub>2</sub> relationship in the SON season was also significant ( $p < 0.001$ ) in the arid desert climate zone but showed a positive relationship. This confirms that the pulsing of NO from the arid soils as soil moisture increases occurs for longer periods in the arid desert than in the arid steppe climate zone. While pulsing occurs heavily in the arid steppe zone, this pulsing was not clearly observed in the arid steppe zone as in the arid desert zone where soil moisture levels are ≤ 20 % (the soil moisture threshold above which tropospheric NO<sub>2</sub> continued to decrease in



the arid steppe climate zone) throughout the year. Feig et al. (2008) found the optimal soil moisture levels for the emission of NO from arid/ semi-arid soils in the Kruger national park in South Africa to be between 10 % and 20 %. With a high percentage of shrublands/grasslands (50 %), the observed relationships between soil moisture NO<sub>2</sub> relationships observed in the arid desert climate zone can be attributed to soil moisture levels which are < 20 % throughout the year and the landcover type found in arid regions as observed by (Feig et al., 2008).

The Granger's causality test was carried out at a lag of one month based on the observed seasonal lag between soil moisture levels and NO<sub>2</sub> especially in the arid zones. Table 1 shows the results of the Granger causality tests for all climate zones. The results showed soil moisture had significant causal effects on NO<sub>2</sub> throughout the 7-year period considered in the arid steppe and arid desert zones. The results for the arid steppe climate zone showed that soil moisture variations affected tropospheric concentrations greatly ( $F = 72.50$ , at  $p < 0.001$ ), the tropospheric NO<sub>2</sub> levels in the West equatorial zone are most influence by soil moisture variability. A strong causality was also observed in the arid desert climate zone ( $F = 72.50$ , at  $p < 0.01$ )

### 3.3 Climate-based NO<sub>2</sub> and soil moisture anomalies, normalised trends and variability

Figure 7 shows the mean monthly anomaly in NO<sub>2</sub> (Figure 7a) and soil moisture (Figure 7b). The displayed anomalies are for May 2008 to April 2014 as a 12 month span (6 months before and after every time step) was used in determining moving averages. The results show a decline in NO<sub>2</sub> in the equatorial monsoon and winter climate zones between May 2008 and August 2009. The arid steppe and arid zones showed increase in NO<sub>2</sub> initially between May and September 2008 and then a decline from October 2008 to August 2009. Sudden negative shifts in the direction of anomaly trends occurred first in the equatorial zones and then 3 months later in the arid zones.

With soil moisture, the most outstanding positive anomaly was observed between July 2008 (-5%) and April 2014 (6%) in the east equatorial monsoon region. Cameroon (located east of Nigeria) released water from the Ladjia dam between July and September 2012 which caused massive flooding in the Niger Delta as the Rivers Benue and Niger overflow their banks (Awhotu, 2015;Tawari-Fufeyin et al., 2015). This may be the main driving factor of the unique soil moisture anomalies (> 5% by 2014) observed in the East equatorial climate zone as the anomalies across all climate zones were similar until August 2012. Soil moisture variations in all climate zones except the east equatorial climate zone remained at  $\pm 4\%$ .

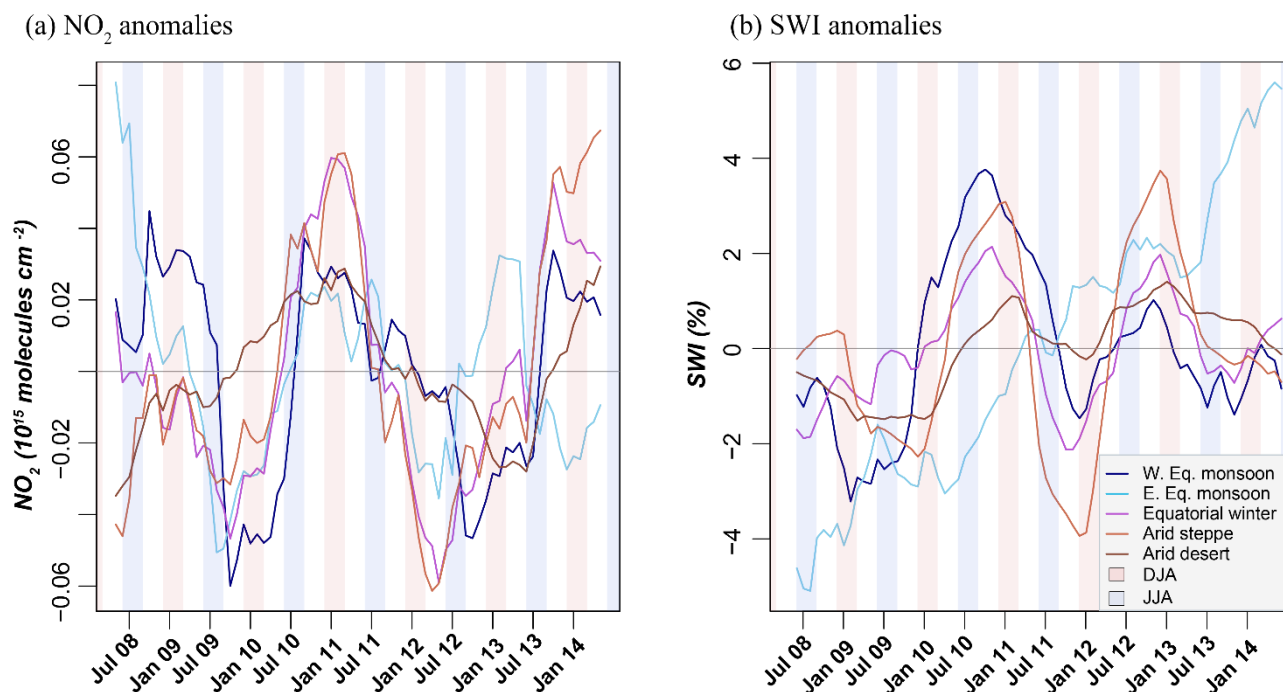


**Figure 7: Anomalies in (a) NO<sub>2</sub> concentrations from OMI and (b) soil moisture Index from ASCAT over West Africa, stratified by climate zones. The annual DJF and JJA seasons are highlighted in red and blue respectively. All monthly anomalies were computed using a 12 month moving average and an overall mean.**

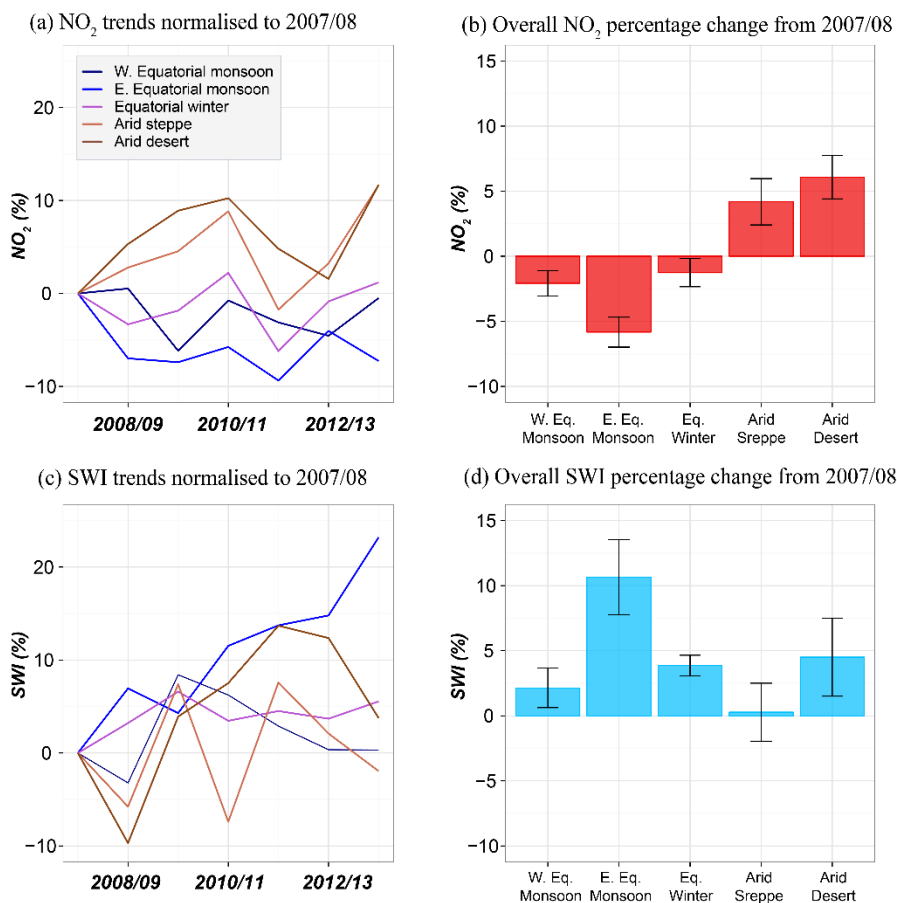
5 The normalised trend analysis for NO<sub>2</sub> and soil moisture showed a likely inverse relationship between NO<sub>2</sub> and soil moisture in the equatorial monsoon and winter climate zones. Figure 8 shows the normalised trends and percentage change for NO<sub>2</sub> (Figure 8a and 8b) and for soil moisture (Figure 7c and 8d). A significant increase in NO<sub>2</sub> in the arid steppe and arid desert zones (> 0.8 %/yr.) was observed between 2007 and 2014. This observed trend compares to observed normalised trends in the arid Middle East by Lelieveld et al. (2015) and Krotkov et al. (2016) in the decade between 2005 and 2015. In both  
 10 climate zones, the difference in soil moisture observed was insignificant (Figure 8d). In the west equatorial and equatorial winter zones, an annual decline in NO<sub>2</sub> of about - 0.5 %/yr. was observed with an increase in soil moisture of ≥ 0.5 %/yr in these zones.

By 2013/14, annual soil moisture in the east equatorial monsoon zone was over 24% higher than it was in 2007/08 (Figure 8c). In addition to the global effect of climate change induced soil moisture variability, the Niger Delta is prone to flooding  
 15 as it is primarily a coastal wetland (Bariweni et al., 2012). The results also indicate that the Ladja dam incident of 2012 had impacts that remained in the east equatorial monsoon climate zone until 2014. This likelihood of flooding in this climate zone is made worse by poor urban planning (Adelye and Rustum, 2011) which results in the obstruction of natural drainage channels. With the current trend in soil moisture levels in the east equatorial monsoon climate region, flooding may remain an annual disaster until more is put in place to improve soil water drainage into the Atlantic.



While a significant rise in  $\text{NO}_2$  was observed in the arid steppe climate zone, the 7-year trend in soil moisture was insignificant. The green wall initiative in Africa which covers most parts of the arid steppe climate zone often referred to as the Sahel and parts of the arid desert zone was launched in 2008 to restore ecosystem productivity and vitality to the Sahel while curbing the southward encroachment of the Sahara (O'Connor and Ford, 2014; Berrahmouni et al., 2014; UNCCD, 2016). Since its inception, the green wall initiative has seen millions of trees planted successfully (Berrahmouni et al., 2014) and others nourished with fertilizers. Fertilizer induced afforestation/agriculture may also affect the abundance of  $\text{NO}_2$  in the arid steppe climate zone as it means the amount of  $\text{NO}_x$  released into the atmosphere after prolonged dry periods due to microbial activities in the soil increases (Robertson et al., 2013). The causal effect of soil moisture on  $\text{NO}_2$  in regions of aridity was shown above. However, the difference in soil moisture and  $\text{NO}_2$  trends in the arid steppe and arid desert climate zones indicate that the  $\text{NO}_2$  trends observed may be connected more with the success of the green wall initiative than with soil moisture variations.

The east equatorial monsoon zone showed the most significant increase in soil moisture at 2%/yr and a corresponding decline in tropospheric  $\text{NO}_2$  concentrations (0.9 %/yr.). The observed decline in tropospheric  $\text{NO}_2$  was 50 % of the magnitude of positive soil moisture trends observed. However, based on the results of the seasonal regression models and Granger's causality tests, the decline in  $\text{NO}_2$  in the east equatorial monsoon zone may not be directly connected to the increase in soil moisture levels. Elvidge et al. (2009) assessed global trends in gas flaring between 1994 and 2008 and found significant decline in gas flaring volumes Nigeria. The authors found that among top gas flaring countries globally, Nigeria had the steepest decline in the volume of gas flared. This declining trend in gas flaring volumes in Nigeria was still evident in 2015 (U.S. Energy Information Administration, 2015)). This may also have causal effects on the observed decline in tropospheric  $\text{NO}_2$  in the east equatorial monsoon region.



5 **Figure 8: Climate-based normalised trends in  $\text{NO}_2$  concentrations and soil moisture index showing (a) the 7 year trend in normalised  $\text{NO}_2$  (b) mean percentage change in  $\text{NO}_2$  (c) the 7 year trend in normalised soil moisture index and (d) mean percentage change in soil moisture between December 2007 and November 2014. The east equatorial monsoon climate zone where most of the Niger Delta is located showed the most decline in  $\text{NO}_2$  ( $> 5\%$ ) and increase in soil moisture levels ( $> 10\%$ ).**

#### 4 Conclusions

Using satellite remote sensed data from OMI and ASCAT, the seasonal fluctuations of tropospheric  $\text{NO}_2$  concentrations and soil moisture levels were analysed over West Africa for several climate zones over a 7-year period (from December 2007 to

10 November 2014). Highest  $\text{NO}_2$  concentrations were observed over densely populated urban areas. The data also showed a North-South gradient in soil moisture levels for the climate zones of West Africa.

In terms of the relationship between soil released  $\text{NO}_2$  and soil moisture, variability in the wet season doesn't seem to just affect observed pulsing in regions of aridity. Soil moisture also plays a vital role in reducing atmospheric  $\text{NO}_2$  in other climate zones between March and May after the biomass burning season. While soil moisture plays a vital role in the sink of

15  $\text{NO}_2$  in the equatorial monsoon and equatorial winter climate zones, Granger causality tests have shown that only regions of



aridity show strong causal effects of soil moisture on tropospheric NO<sub>2</sub> in West Africa. The results have shown that the causal effect of soil moisture trends may not be directly responsible for the observed increasing NO<sub>2</sub> trends in the arid steppe and arid desert climate zones.

The great green wall initiative in the Sahel will reduce deforestation, desert encroachment and boost the productivity of the Sahel ecosystem. So far, the initiative has focused more on tree planting. O'Connor and Ford (2014) propose that planting shrubs which will improve grazing areas by Nitrogen fixation rather than trees may have a more sustainable approach to the initiative. Nitrogen fertilizer application methods that reduce the formation of NO<sub>x</sub> from soil processes are used in the USA (Robertson et al., 2013). More in-situ research needs to go into assessing what the long term impacts of this green wall afforestation with strong N fertilizer inputs will be on soil NO<sub>x</sub> pulsing and the atmospheric chemistry of the West African Sahel and globally and then mitigating the inherent climate change related risks.

A significant increase in soil moisture occurred over the 7-year period analysed with a corresponding decline in NO<sub>2</sub> concentrations in the east equatorial monsoon zone where the Niger Delta is located. The satellite data analysis indicates that variability in soil moisture anomalies likely affects seasonal tropospheric NO<sub>2</sub> concentrations in humid/monsoonal areas. This needs to be investigated more using in-situ time series. The availability of soil moisture data over the humid east equatorial monsoon zone from the ASCAT sensor on the MetOp-A satellite means that for many years to come, the effect of soil moisture on NO<sub>2</sub> over this area can be studied in closer detail with longer time series.

### Data Availability

The OMI NO<sub>2</sub> data set (OMNO2d) used in this research is provided by the NASA GES DISC team is available at <http://mirador.gsfc.nasa.gov/>. The ASCAT SWI data set is provided by the COPERNICUS/ASCAT team and is available at <http://land.copernicus.vgt.vito.be>. The ESA GLOBCOVER 2009 data is available at [http://due.esrin.esa.int/page\\_globcover.php](http://due.esrin.esa.int/page_globcover.php) and the Koppen-Geiger climate classification data at <http://koeppen-geiger.vu-wien.ac.at/present.htm>.

### Acknowledgments

Ajoke Onojeghuo was funded by the Niger Delta Development Corporation (NDDC). Heiko Balzter was supported by the Royal Society Wolfson Research Merit Award, 2011/R3 and the NERC National Centre for Earth Observation.



## Author contribution

Ajoke Onojeghwo prepared the model codes in R with inputs from Heiko Balzter and Paul Monks. Ajoke Onojeghwo prepared the manuscript with input from co-authors.

## Competing interests

- 5 The authors declare that they have no conflict of interest.

## References

- Adelye, A., and Rustum, R.: Flooding influence of Urban Planning. *J. Urban Design & Planning* 164, 175-187, 2011.
- Awhotu, E.: The unending wave of floods, in: Peoples Daily, People's media limited, 2015.
- 10 Bariweni, P. A., Tawari, C. C., and Abowei, J. F. N.: Some Environmental Effects of Flooding in the Niger Delta Region of Nigeria, *International Journal of Fisheries and Aquatic Sciences*, 1, 2012.
- Basara, J. B., and Crawford, K. C.: Linear relationships between root-zone soil moisture and atmospheric processes in the planetary boundary layer, *Journal of Geophysical Research: Atmospheres*, 107, ACL 10-11-ACL 10-18, 10.1029/2001JD000633, 2002.
- 15 Batello, C., Marzot, M., and Touré, A. H.: The future of an ancient lake, *FAO Interdepartmental Working Group on Biological Diversity for Food and Agriculture*, Rome ISBN 92-5-105064-3, 2004.
- Berrahmouni, N., Tapsoba, F., and Berte, C. J.: The Great Green Wall for the Sahara and the Sahel Initiative: building resilient landscapes in African drylands, *GENETIC CONSIDERATIONS IN ECOSYSTEM RESTORATION USING NATIVE TREE SPECIES*, 15, 2014.
- Bontemps, S., Defourny, P., Van Bogaert, E., Oliver, A., and Vasileios, K.: *GLOBCOVER 2009 Product Description Manual*, in, edited by: Louvian, U. C. d., ESA CCI, 2010.
- 20 Breheny, P., and Burchett, W.: Visualization of Regression Models using visreg, in, University of Kentucky, Lexington, KY, 2013.
- Brocca, L., Melone, F., Moramarco, T., Wagner, W., and Hasenauer, S.: ASCAT soil wetness index validation through in situ and modeled soil moisture data in central Italy, *Remote Sensing of Environment*, 114, 2745-2755, <http://dx.doi.org/10.1016/j.rse.2010.06.009>, 2010.
- 25 Chen, J., Jönsson, P., Tamura, M., Gu, Z., Matsushita, B., and Eklundh, L.: A simple method for reconstructing a high-quality NDVI time-series data set based on the Savitzky–Golay filter, *Remote Sensing of Environment*, 91, 332-344, <http://dx.doi.org/10.1016/j.rse.2004.03.014>, 2004.
- Chen, L. W. A., Verburg, P., Shackelford, A., Zhu, D., Susfalk, R., Chow, J. C., and Watson, J. G.: Moisture effects on carbon and nitrogen emission from burning of wildland biomass, *Atmos. Chem. Phys.*, 10, 6617-6625, 10.5194/acp-10-6617-2010, 2010.
- 30 Conway, G.: The science of climate change in Africa: impacts and adaptation, in, edited by: Change, G. I. f. C., Imperial College, London, London, 2009.
- Delon, C., Reeves, C. E., Stewart, D. J., Serça, D., Dupont, R., Mari, C., Chaboureaud, J. P., and Tulet, P.: Biogenic nitrogen oxide emissions from soils &ndash; impact on NO<sub>x</sub> and ozone over West Africa during AMMA (African Monsoon Multidisciplinary Experiment): modelling study, *Atmos. Chem. Phys.*, 8, 2351-2363, 10.5194/acp-8-2351-2008, 2008.
- 35 Delon, C., Mougin, E., Serca, D., Grippa, M., Hiernaux, P., Diawara, M., Galy-Lacaux, C., and Kergoat, L.: Modelling the effect of soil moisture and organic matter degradation on biogenic NO emissions from soils in Sahel rangeland (Mali), *Biogeosciences*, 12, 1155-1203, 2015.
- Eltahir, E. A. B., and Gong, C.: Dynamics of Wet and Dry Years in West Africa, *Journal of Climate*, 6, 1002-1008, 1996.
- Elvidge, C., Ziskin, D., Baugh, K., Tuttle, B., Ghosh, T., Pack, D., Erwin, E., and Zhizhin, M.: A Fifteen Year Record of Global Natural Gas Flaring Derived from Satellite Data, *Energies*, 2, 595, 2009.
- 40 Erasmi, S., Bothe, M., and Petta, R. A.: Enhanced filtering of MODIS time series data for the analysis of Desertification processes in North east Brazil, *Proceedings of the ISPRS/ITC-Midterm Symposium—Remote Sensing: From Pixels to Processes*, Enschede, The Netherlands, 2006.
- FAO: Integrating crops and livestock in West Africa, Agriculture and Consumer Protection, Food and Agriculture Organisation, Benin, 112 pp., 1983.
- 45 Feig, G. T., Mamtimin, B., and Meixner, F. X.: Soil biogenic emissions of nitric oxide from a semi-arid savanna in South Africa, *Biogeosciences*, 5, 1723-1738, 10.5194/bg-5-1723-2008, 2008.



- Fischer, B., and Pau, G.: Package 'rhd5': HDF5 interface to R, in: Bioconductor, 2015.
- GCOS: Status of the global observing system for climate, World Meteorological Organization, Geneva, 2015.
- Grajales, J. F., and Baquero-Bernal, A.: Inference of surface concentrations of nitrogen dioxide (NO<sub>2</sub>) in Colombia from tropospheric columns of the ozone measurement instrument (OMI), *Atmósfera*, 27, 193-214, [http://dx.doi.org/10.1016/S0187-6236\(14\)71110-5](http://dx.doi.org/10.1016/S0187-6236(14)71110-5), 2014.
- 5 Granger, C. W. J.: Investigating Causal Relations by Econometric Models and Cross-spectral Methods, *Econometrica*, 37, 424-438, 1969.
- Hijmans, R. J.: Introduction to the 'raster' package (version 2.3-40), in, 2015.
- Hopkins, J. R., Evans, M. J., Lee, J. D., Lewis, A. C., H Marsham, J., McQuaid, J. B., Parker, D. J., Stewart, D. J., Reeves, C. E., and Purvis, R. M.: Direct estimates of emissions from the megacity of Lagos, *Atmos. Chem. Phys.*, 9, 8471-8477, 10.5194/acp-9-8471-2009, 2009.
- 10 Hoscilo, A., Balzter, H., Bartholomé, E., Boschetti, M., Brivio, P. A., Brink, A., Clerici, M., and Pekel, J. F.: A conceptual model for assessing rainfall and vegetation trends in sub-Saharan Africa from satellite data, *International Journal of Climatology*, 10, 10.1002/joc.4231, 2015.
- Hothorn, T., Zeileis, A., Farebrother, R. W., Cummins, C., Millo, G., and Mitchell, D.: *lmtest: Testing linear regression models*, 2014.
- Hudman, R. C., Russell, A. R., Valin, L. C., and Cohen, R. C.: Interannual variability in soil nitric oxide emissions over the United States as viewed from space, *Atmos. Chem. Phys.*, 10, 9943-9952, 10.5194/acp-10-9943-2010, 2010.
- 15 Hudman, R. C., Moore, N. E., Mebust, A. K., Martin, R. V., Russell, A. R., Valin, L. C., and Cohen, R. C.: Steps towards a mechanistic model of global soil nitric oxide emissions: implementation and space based-constraints, *Atmos. Chem. Phys.*, 12, 7779-7795, 10.5194/acp-12-7779-2012, 2012.
- Ibrahim, Y. Z., Balzter, H., Kaduk, J., and Tucker, C. J.: Land Degradation Assessment Using Residual Trend Analysis of GIMMS NDVI3g, Soil Moisture and Rainfall in Sub-Saharan West Africa from 1982 to 2012, *Remote Sensing*, 7, 5471-5494, 10.3390/rs70505471, 2015.
- 20 IPCC: *Climate Change 2007: The Physical Science Basis*, in, edited by: Change, W. G. I. o. t. I. P. o. C., Cambridge University Press, Cambridge, 996, 2007.
- Jaegle, L., Steinberger, L., Martin, R. V., and Chance, K.: Global partitioning of NO<sub>x</sub> sources using satellite observations: Relative roles of fossil fuel combustion, biomass burning and soil emissions, *Faraday Discuss*, 130, 407-423, 2005.
- 25 Jaegle, L., Steinberger, L., Martin, R. V., and Chance, K.: Global partitioning of NO<sub>x</sub> sources using satellite observations: Relative roles of fossil fuel combustion, biomass burning and soil emissions, *Faraday Discuss*, 130, 407-423, 2005.
- Keller, M., and Reiners, W. A.: Soil-atmosphere exchange of nitrous oxide, nitric oxide, and methane under secondary succession of pasture to forest in the Atlantic lowlands of Costa Rica, *Global Biogeochemical Cycles*, 8, 399-409, 10.1029/94GB01660, 1994.
- 30 Ker, A.: *Farming Systems Of The African Savanna*; A Continent In Crisis, IDRC, 1995.
- Kidd, R., Makhmara, H., and Paulik, C.: Product User Manual (Soil Water Index (Swi) – Version 2.0, Surface State Flag (Ssf) – Version 2.0), in: *Gio Global Land Component - Lot I "Operation of the Global Land Component"*, edited by: Operations, G. I., 2014.
- Kim, D.-G., Vargas, R., Bond-Lamberty, B., and Turetsky, M. R.: Effects of soil rewetting and thawing on soil gas fluxes: a review of current literature and suggestions for future research, *Biogeosciences*, 9, 2459-2483, 2012.
- 35 Kottke, M., Grieser, J., Beck, C., Rudolf, B., and Rubel, F.: World Map of the Köppen-Geiger climate classification updated, *Meteorologische Zeitschrift*, 15, 259-263, 10.1127/0941-2948/2006/0130, 2006.
- Krotkov, N. A., McLinden, C. A., Li, C., Lamsal, L. N., Celarier, E. A., Marchenko, S. V., Swartz, W. H., Bucsele, E. J., Joiner, J., Duncan, B. N., Boersma, K. F., Veefkind, J. P., Levelt, P. F., Fioletov, V. E., Dickerson, R. R., He, H., Lu, Z., and Streets, D. G.: Aura OMI observations of regional SO<sub>2</sub> and NO<sub>2</sub> pollution changes from 2005 to 2015, *Atmos. Chem. Phys.*, 16, 4605-4629, 10.5194/acp-16-4605-2016, 2016.
- 40 Lamsal, L. N., Krotkov, N. A., Celarier, E. A., Swartz, W. H., Pickering, K. E., Bucsele, E. J., Gleason, J. F., Martin, R. V., Philip, S., Irie, H., Cede, A., Herman, J., Weinheimer, A., Szykman, J. J., and Knepp, T. N.: Evaluation of OMI operational standard NO<sub>2</sub> column retrievals using in situ and surface-based NO<sub>2</sub> observations, *Atmos. Chem. Phys.*, 14, 11587-11609, 10.5194/acp-14-11587-2014, 2014.
- 45 Lehsten, V., Tansey, K., Balzter, H., Thonicke, K., Spessa, A., Weber, U., Smith, B., and Arneith, A.: Estimating carbon emissions from African wildfires, *Biogeosciences*, 6, 349-360, 10.5194/bg-6-349-2009, 2009.
- Lelieveld, J., Beirle, S., Hörmann, C., Stenchikov, G., and Wagner, T.: Abrupt recent trend changes in atmospheric nitrogen dioxide over the Middle East, *Science Advances*, 1, e1500498, 10.1126/sciadv.1500498, 2015.
- Levelt, P. F., Van den Oord, G. H. J., Dobber, M. R., Malkki, A., Huib, V., de Vries, J., Stammes, P., Lundell, J. O. V., and Saari, H.: The ozone monitoring instrument, *Geoscience and Remote Sensing, IEEE Transactions on*, 44, 1093-1101, 10.1109/TGRS.2006.872333, 2006.
- 50 Meixner, F., and Yang, W. X.: Biogenic emissions of nitric oxide and nitrous oxide from arid and semi-arid land, in: *Dryland ecohydrology*, Springer, 233-255, 2006.
- Monks, P. S.: Gas-phase radical chemistry in the troposphere, *Chemical Society Reviews*, 34, 376-395, 10.1039/B307982C, 2005.
- Monks, P. S., and Beirle, S.: Applications of Satellite Observations of Tropospheric composition, in: *The Remote Sensing of Tropospheric Composition from Space*, edited by: Burrows, J. P., Platt, U., and Borell, P., *Physics of Earth and Space Environments*, Springer Berlin, 365-418, 2011.
- 55



- Monks, P. S., Archibald, A. T., Colette, A., Cooper, O., Coyle, M., Derwent, R., Fowler, D., Granier, C., Law, K. S., Mills, G. E., Stevenson, D. S., Tarasova, O., Thouret, V., von Schneidemesser, E., Sommariva, R., Wild, O., and Williams, M. L.: Tropospheric ozone and its precursors from the urban to the global scale from air quality to short-lived climate forcer, *Atmos. Chem. Phys.*, 15, 8889-8973, 10.5194/acp-15-8889-2015, 2015.
- 5 N'Datchoh, E. T., Konaré, A., Diedhiou, A., Diawara, A., Quansah, E., and Assamoi, P.: Effects of climate variability on savannah fire regimes in West Africa, *Earth System Dynamics*, 6, 161-174, 10.5194/esd-6-161-2015, 2015.
- O'Connor, D., and Ford, J.: Increasing the Effectiveness of the "Great Green Wall" as an Adaptation to the Effects of Climate Change and Desertification in the Sahel, *Sustainability*, 6, 7142-7154, 2014.
- Oetjen, H., Baidar, S., Krotkov, N. A., Lamsal, L. N., Lechner, M., and Volkamer, R.: Airborne MAX-DOAS measurements over  
 10 California: Testing the NASA OMI tropospheric NO<sub>2</sub> product, *Journal of Geophysical Research-Atmospheres*, 118, 7400-7413, 10.1002/jgrd.50550, 2013.
- OMI-NO2-Algorithm-Team: OMNO2 README File, in, edited by: Center, N. G. S. F., 2013.
- Paulik, C., Dorigo, W., Wagner, W., and Kidd, R.: Validation of the ASCAT Soil Water Index using in situ data from the International Soil Moisture Network, *International Journal of Applied Earth Observation and Geoinformation*, 30, 1-8,  
 15 <http://dx.doi.org/10.1016/j.jag.2014.01.007>, 2014.
- Pearl, J.: *Causality: Models, reasoning, and inference*, Cambridge University Press, 2000.
- Pierce, D.: Package "ncdf4": Interface to Unidata netCDF (version 4 or earlier) format data files, 2015.
- Pilegaard, K.: Processes regulating nitric oxide emissions from soils, *Philosophical Transactions of the Royal Society of London B: Biological Sciences*, 368, 10.1098/rstb.2013.0126, 2013.
- 20 Pradier, S., Jean-Luc, A., Chong, M., Escobar, J., Peuch, V.-H., Lamarque, J.-F., Khattatov, B., and Edwards, D.: Evaluation of 2001 springtime CO transport over West Africa using MOPITT CO measurements assimilated in a global chemistry transport model, *Tellus B*, 58, 163-176, 10.1111/j.1600-0889.2006.00185.x, 2006.
- Richter, A., Burrows, J. P., Nusz, H., Granier, C., and Niemeier, U.: Increase in tropospheric nitrogen dioxide over China observed from space, *Nature*, 437, 129-132, [http://www.nature.com/nature/journal/v437/n7055/supinfo/nature04092\\_S1.html](http://www.nature.com/nature/journal/v437/n7055/supinfo/nature04092_S1.html), 2005.
- 25 Robertson, G. P., Bruulsema, T. W., Gehl, R. J., Kanter, D., Mauzerall, D. L., Rotz, C. A., and Williams, C. O.: Nitrogen-climate interactions in US agriculture, *Biogeochemistry*, 114, 41-70, 10.1007/s10533-012-9802-4, 2013.
- Sarkar, D.: Package "lattice", in, 2015.
- Savitzky, A., and Golay, M. J. E.: Smoothing and differentiation by simplified least squares procedures, *Anal. Chem.*, 36, 1672-1639, 1964.
- 30 Schwela, D.: AQM Status in Western and Central Africa: Evidence of Health Effects and Links to Climate Change, West and Central Africa Sub-Regional Workshop on Better Air Quality Policy Session: July 20-21, 2009 Abidjan, Côte d'Ivoire 2009.
- Stevens, A., and Ramirez-Lopez, L.: An introduction to the prospectr package, in: R, 2014.
- Sugihira, G., May, R., Ye, H., Hsieh, C.-h., Deyle, E., Fogarty, M., and Munch, S.: Detecting Causality in Complex Ecosystems, *Science*, 368, 496-500, 2012.
- 35 Tawari-Fufeyin, P., Paul, M., and Godleads, A. O.: Some Aspects of a Historic Flooding in Nigeria and Its Effects on some Niger-Delta Communities, *American Journal of Water Resources*, 3, 7-16, 10.12691/ajwr-3-1-2, 2015.
- The R Core Team: R: A Language and Environment for Statistical Computing, in, R Foundation for Statistical Computing, Vienna, Austria, 2014.
- Thornley, D. J.: Novel Anisotropic Multidimensional Convolutional Filters for Derivative Estimation and Reconstruction, *Signal Processing and Communications*, 2007. ICSPC 2007. IEEE International Conference on, 2007, 253-256.
- 40 Tschakert, P., Sagoe, R., Ofori-Darko, G., and Codjoe, S. N.: Floods in the Sahel: an analysis of anomalies, memory, and anticipatory learning, *Climate change*, 103, 471 - 502, 10.1007/s10584-009-9776-y, 2010.
- International Energy Statistics: <http://www.eia.gov/beta/international/>, access: 16th of October, 2015, 2015.
- The Great Green Wall for the Sahara and the Sahel Initiative: <http://www.global-mechanism.org/content/great-green-wall-sahara-and-sahel-initiative>, access: 23/11/2016, 2016.
- 45 von Schneidemesser, E., Monks, P. S., Allan, J. D., Bruhwiler, L., Forster, P., Fowler, D., Lauer, A., Morgan, W. T., Paasonen, P., Righi, M., Sindelarova, K., and Sutton, M. A.: Chemistry and the Linkages between Air Quality and Climate Change, *Chemical Reviews*, 115, 3856-3897, 10.1021/acs.chemrev.5b00089, 2015.
- Wagner, W., Hahn, S., Kidd, R., Melzer, T., Bartalis, Z., Hasenauer, S., Figa-Saldaña, J., de Rosnay, P., Jann, A., Schneider, S., Komma, J., Kubu, G., Brugger, K., Aubrecht, C., Züger, J., Gangkofner, U., Kienberger, S., Brocca, L., Wang, Y., Blöschl, G., Eitzinger, J., Steinnocher, K., Zeil, P., and Rubel, F.: The ASCAT Soil Moisture Product: A Review of its Specifications, Validation Results, and Emerging Applications, *Meteorologische Zeitschrift*, 22, 5-33, 10.1127/0941-2948/2013/0399, 2013.
- 50 Wai, K. M., Wu, S., Kumar, A., and Liao, H.: Seasonal variability and long-term evolution of tropospheric composition in the tropics and Southern Hemisphere, *Atmos. Chem. Phys.*, 14, 4859-4874, 2014.
- 55 Zeileis, A., and Grothendieck, G.: zoo: S3 Infrastructure for Regular and Irregular Time Series, *Journal of Statistical software*, 14, 2005.



**Table 1. Results of the Climate based Grangers causality test for the effect of soil moisture variability on tropospheric NO<sub>2</sub> concentrations.**

	<b>West equatorial monsoon</b>	<b>East equatorial monsoon</b>	<b>Equatorial Winter</b>	<b>Arid steppe</b>	<b>Arid desert</b>
<b>F statistic</b>	2.19	0.001	0.04	72.50***	10.22**

5